

# Role of spurious reflections in ring-down spectroscopy

R. W. Fox and L. Hollberg

National Institute of Standards and Technology, 325 Broadway, Boulder, Colorado 80305

Received April 23, 2002

Spurious coherent reflections from optical elements that re-enter an exit port of a two-mirror ring-down cavity can significantly change the effective reflectivity of the cavity mirrors, thus altering the cavity decay time. For a 25-cm-long Fabry–Perot cavity with a decay constant of 40  $\mu\text{s}$ , we find that a specular reflection of only  $10^{-4}$  of the transmitted ring-down power that is mode matched back toward the cavity could change the decay time by as much as  $\pm 0.4 \mu\text{s}$ , depending on the phase of the returning reflection. The perturbation of the decay time is proportional to the electric field, so a decrease in the spurious reflected power of 100 times will result in a perturbation that is only 10 times smaller. We demonstrate the effect with a cw system by purposely introducing a spurious reflection.

OCIS codes: 120.6200, 140.4780, 300.1030.

Spurious reflections from optical elements in the beam path have often been cited as the limitation to achieving lower detection limits with laser-spectroscopic methods.<sup>1</sup> In the standard technique of rf absorption spectroscopy, the interference fringes form a wavelength-, temperature-, and vibration-dependent baseline of the power detected at the modulation frequency. The use of multiple-layer antireflection-coated optics and diligent attention to specular reflections and beam scatter all help reduce the problem, but spurious reflections are quite difficult to eliminate entirely. A number of methods have been proposed and utilized over the years to reduce the effect, usually by forcing the unwanted interference to cycle through fringes and subsequently averaging.<sup>2</sup>

The technique of cavity ring-down spectroscopy has been successfully used in many experiments to take advantage of the long absorption path length in high-finesse optical resonators. Although the majority of published cavity decay measurements have utilized pulsed lasers, it has been long recognized that using cw lasers may yield superior results.<sup>3</sup> In particular, cw lasers were used in some of the most sensitive experiments to date,<sup>4–6</sup> which involved frequency locking of lasers to the ring-down cavities. Although impressive, none of these experiments reached the fundamental limits set by the inherent shot noise of the light. However, to our knowledge, the deleterious effects of spurious reflections have not been discussed and could account for some of the discrepancy between the reported results and the fundamental limits. Spurious reflections could also affect cavity ring-down spectroscopy experiments employing pulsed lasers. Regardless of the light source, a cavity decay measurement may be corrupted if a spurious reflection or scatter from a beam exiting a cavity re-enters the cavity and interferes coherently with the cavity wave.

The loss in an optical cavity may be separated into loss that is due to the finite transmission of the mirrors, mirror scatter and absorption, and intracavity absorption. Neglecting the relatively small mirror scatter and absorption, so that  $T \cong 1 - R$ , one may deduce the rate of loss,  $\tau^{-1}$ , from the round-trip loss divided by the round-trip time<sup>7</sup>:

$$\tau^{-1} = \frac{[\alpha L + \sum_{i=1}^k (1 - R_i)]}{nL/c}, \quad (1)$$

where the intracavity loss  $\alpha$  is in inverse centimeters,  $nL$  is the optical round-trip length in centimeters, and  $R_i$  is the power reflectivity of the  $i$ th mirror. Here we assume that the intracavity absorber fills the space between the mirrors. From Eq. (1) we may obtain the sensitivity of the power decay time constant to the intracavity absorption constant,

$$\frac{d\tau}{d\alpha} = -\frac{c}{n} \tau^2, \quad (2)$$

and also the intracavity absorption in terms of the decay time constant with and without the absorber present,

$$\alpha = \frac{n}{c} \left( \frac{1}{\tau} - \frac{1}{\tau_0} \right). \quad (3)$$

We use our 25-cm-long ( $L = 50$  cm) two-mirror cavity with  $R_1 = R_2$  and a  $\tau \approx 40 \mu\text{s}$  decay constant as an example to illustrate the problem of spurious reflections perturbing a decay measurement. Such a cavity has an absorption sensitivity, according to the inverse of Eq. (2), of  $d\alpha/d\tau \sim 2 \times 10^{-8} \text{ cm}^{-1}/\mu\text{s}$ . The mirrors have a reflectivity  $R$  of approximately 0.999979. This reflectivity is obtained with a high-order thin-film design similar to that depicted in Fig. 1. The high reflectivity experienced by the cavity wave is due to the constructive interference of the reflections from each thin-film layer interface. However, the resultant reflectance of the cavity wave is also a function of what happens to the transmitted beam. If a fraction of this beam is returned to the cavity mode, the resultant field reflected from the mirror will be affected. It is the reflectance (reflected power/incident power), which is in fact the effective reflectivity, that is affected. For instance, whether the mirror is antireflection coated or not, the residual reflection from the back side of each high-finesse mirror will contribute a term that will manifest itself on the cavity time constant as a wavelength- (and temperature-) dependent cyclical baseline. However, other reflections from objects beyond the substrate's back side are just as capable of changing the effective reflectivity and the subsequent cavity decay time constant. Such

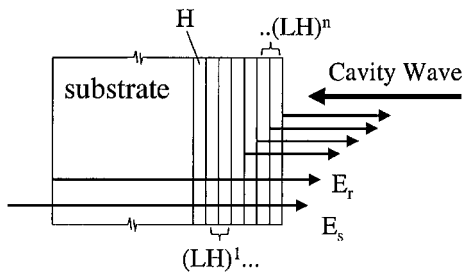


Fig. 1. Typical thin-film high-finesse mirror with the intracavity wave incident from the right. L and H refer to layers whose relative refraction index is low or high, respectively. The resultant reflection is determined by the coherent superposition of the individual reflections, including the back-surface reflection ( $E_r$ ) and reflections from surfaces some distance away, as designated by  $E_s$ . Back-surface reflections may be avoided by angle polishing of the substrate.

reflections will cause the cavity decay time constant to depend on air currents, vibration, and temperature external to the cavity, since these items will modulate the phase of the returning light.

We analyzed this problem for our cavity by using thin-film design software to calculate the change in effective reflectivity caused by an interface some distance away from the thin-film stack. The index change at the interface was used to provide an adjustable reflection, the magnitude of which could be calculated from the Fresnel equations. Not surprisingly, the resultant mirror reflectivity plot versus wavelength clearly shows interference fringes with a period  $c/2nl$ , where  $l$  is the distance to the interface. Maximum and minimum deviations from the nominal reflectivity (which could be caused by variation of either  $\lambda$  or  $l$ ) were taken from these plots. The corresponding maximum deviations to be expected in the cavity decay time were then calculated with Eq. (1), with the nominal thin-film reflectivity for  $R_1$  and the modified reflectivity for  $R_2$ . Plotted in Fig. 2 are the maximum deviations in the mirror's effective reflectivity from the nominal value caused by a given fraction of power reflected back toward the cavity exit port. The resultant effective reflectivity experienced by the cavity wave can be anything between these two extremes, depending on the relative phase of the spurious reflection. Furthermore, since it is a fraction of the transmitted cavity wave that is retroreflected back that is perturbing the effective reflectivity of the high-finesse mirror, the perturbation is constant throughout the cavity decay, as long as the relative phase of the return light is constant. The resulting change in the time constant is also shown in Fig. 2. Although the reflectivity bounds are shown as two curves (since for large spurious retroreflections they are different), the positive- and negative-reflectivity bounds correspond to nearly symmetrical deviations from the nominal decay constant. Consequently, only one curve is shown, and it is labeled  $\pm$  maximum deviation from the nominal decay.

A cyclical baseline that is due to the back surface of the high-finesse mirror substrate is the most obvious example of this effect. Our two mirrors are fused

silica, approximately 4 mm thick, each of which should independently contribute a 25-GHz ( $0.83\text{-cm}^{-1}$ ) period to the baseline of the cavity's decay constant. The contributions will tend to enhance or cancel each other out, depending on the phases of the returning back-surface reflections relative to the cavity wave. The cyclical baseline is temperature dependent ( $\sim 2.7\text{ GHz}/^\circ\text{C}$  or  $0.09\text{ cm}^{-1}/^\circ\text{C}$ ) because of the temperature dependence of the fused-silica refractive index and length. Figure 3 is an extreme example, in which the contributions to the cyclical baseline of two mirrors with uncoated substrates are partially in phase with each other. From Fig. 2, we expect the maximum change in the cavity decay time constant that is due to each mirror to be  $\pm 7.4\ \mu\text{s}$ , or a potential deviation from the nominal cavity decay time by as much as  $\pm 14.8\ \mu\text{s}$ . The measured change is  $\sim \pm 5.5\ \mu\text{s}$ , indicating that the effect of the two back-surface reflections on the cavity finesse may be partially out of phase.

We demonstrate this effect of spurious reflections affecting the cavity decay time by introducing a small external reflection, while varying the distance from the reflector to the cavity. A beam splitter ( $R = 5.5\%$ ) was installed before the detector used to monitor the cavity transmission. The beam-splitter reflection was retroreflected by a flat mirror ( $R \sim 99\%$ ) mounted on a piezoelectric transducer. A neutral-density filter ( $T = 50\%$ ) was used in front of the mirror so that approximately  $7.5 \times 10^{-4}$  of the decaying cavity power was reflected back to the cavity. However, the reflected beam was not mode matched to the cavity, since the beam from the cavity was expanding from the cavity waist, whereas the reflection back to the cavity was from a flat mirror. Consequently, the actual fraction of power coupled back into the cavity mode should be

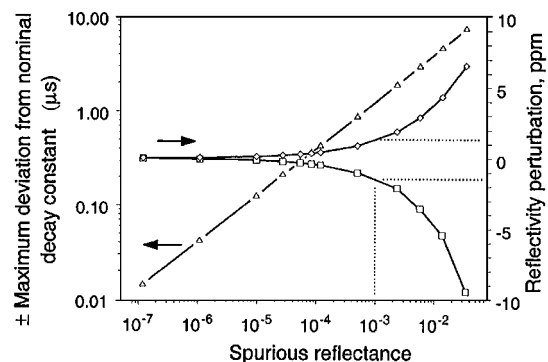


Fig. 2. Curves marked with squares and diamonds, calculated maximum deviations of the apparent reflectivity of the high-finesse mirror, caused by a retroreflection of a fraction of the beam transmitted from the cavity. For instance, a mode-matched retroreflection of  $10^{-3}$  will change the effective reflectivity by  $-1.4$  to  $+1.4$  parts in  $10^6$  (ppm), depending on the relative phase of the returning light (dotted lines). The corresponding change of the ring-down time constant for such a retroreflection entering one port, assuming a two-mirror cavity, a round-trip cavity length of 50 cm, and a nominal decay constant of  $40\ \mu\text{s}$ , is shown by the line marked with triangles. That change would be approximately  $\pm 1\ \mu\text{s}$  for a spurious retroreflection of  $10^{-3}$ , equivalent to an apparent change of an intracavity absorption of  $\pm 2 \times 10^{-8}\text{ cm}^{-1}$ .

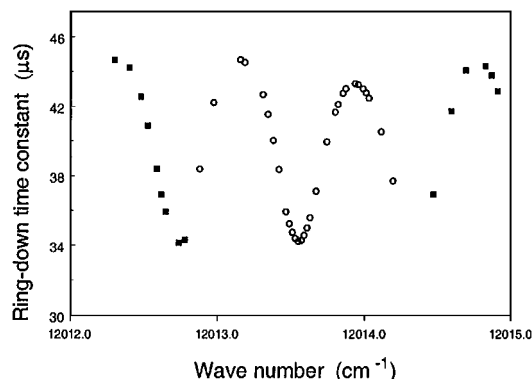


Fig. 3. Measured time constants of a two-mirror cavity with no antireflection coating on either mirror's back surface. Each point is the exponential time constant determined from a fit of the ring-down signal of a  $TEM_{00}$  mode. The open circles were obtained on day 1, and the data indicated by the squares were from the following day. A reflectivity of 3.4% is expected at the fused-silica-air interfaces. From Fig. 2, we expect a maximum perturbation from each mirror of  $\pm 7.4 \mu\text{s}$ . The data show a perturbation of the total cavity time constant of  $\pm 5.5 \mu\text{s}$ , consistent with a partial cancellation of the contribution from each mirror because of a slight difference in mirror thickness.

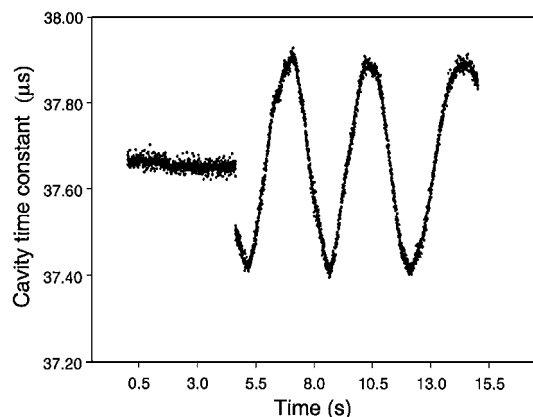


Fig. 4. Measurement of 3000 sequential cavity decay time constants. Each point represents a time constant determined by an exponential fit to  $175 \mu\text{s}$  of a decay from a  $TEM_{00}$  mode. The laser is then relocked to the same mode, and the next decay is triggered approximately 5 ms later. At 4.5 s into the data set, a spurious reflection of  $7.5 \times 10^{-4}$  was introduced by means of unblocking a piezoelectric transducer-mounted mirror positioned 50 cm from the cavity. The mirror motion is unidirectional (toward the cavity) for the entire data set. The data show a deviation of the ring-down time constant that is due to the spurious reflection of  $\pm 0.25 \mu\text{s}$ , which is consistent with an expected deviation of  $\pm 1 \mu\text{s}$  that should occur from a mode-matched reflection, as shown by Fig. 2.

somewhat less than  $7.5 \times 10^{-4}$ , which is consistent with the data in Fig. 4.

The cavity decay times were measured by means of locking an extended-cavity diode laser to the high-finesse cavity by use of the Pound-Drever-Hall technique<sup>8</sup> and subsequent unlocking of the laser while the cavity transmission was monitored. At each unlock-

ing event, the Pound-Drever-Hall modulation sidebands were turned off and the laser frequency was quickly tuned by a few megahertz so that the incident laser power did not affect the decay from the transmission port. This approach couples the light efficiently to the cavity and results in very reproducible data. It requires that the first several microseconds of data be neglected but avoids the need for an acousto-optic modulator.

Although we have not investigated ring cavities in this Letter, spurious reflections are likely to be less of a problem than with two-mirror Fabry-Perot cavities. This is because the reflection must come from the reverse-going cavity mode, which is usually weak since it is driven only by mirror scattering.

In summary, we have identified spurious optical reflections as a potential source of noise in cavity ring-down spectroscopy measurements. The effect can be significant: Even a single reflection from a V-layer antireflection coating ( $R \sim 0.25\%$ ) returned to the cavity used in this Letter can cause a systematic error in the measured absorption of parts in  $10^{-8}$ , far above the random noise limit. Furthermore, air currents and temperature-induced motion will limit the usefulness of averaging multiple cavity decay measurements, since the induced systematic error is interferometrically dependent on the optical path length from the spurious reflector to the cavity. Attention to possible scatter and reflection sources should reduce the systematic deviations of the decay measurements. However, it is likely that the best results will be obtained with an active solution such as the use of piezoelectric transducer-mounted mirrors outside the cavity to modulate the distance to any spurious reflections. The induced error is cyclical and will be randomized by varying the optical path length back to the cavity.<sup>2</sup> In such instances, the variance of each data set is increased, but subsequent averaging results in superior repeatability.

The authors are grateful to V. L. Velichansky for helpful discussions. R. W. Fox's e-mail address is richard.fox@nist.gov.

## References

1. P. Kluczynski, J. Gustafsson, A. M. Lindberg, and O. Axner, *Spectrochim. Acta B* **56**, 1277 (2001), and references therein.
2. C. R. Webster, *J. Opt. Soc. Am. B* **2**, 1464 (1985).
3. P. Zalicki and R. N. Zare, *J. Chem. Phys.* **102**, 2708 (1995).
4. T. G. Spence, C. C. Harb, B. A. Paldus, R. N. Zare, B. Wilke, and R. L. Byer, *Rev. Sci. Instrum.* **71**, 347 (2000).
5. J. Ye and J. L. Hall, *Phys. Rev. A* **61**, 061802(R) (2000).
6. M. D. Levenson, B. A. Paldus, T. G. Spence, C. C. Harb, R. N. Zare, M. J. Lawrence, and R. L. Byer, *Opt. Lett.* **25**, 920 (2000).
7. M. D. Levenson, B. A. Paldus, T. G. Spence, C. C. Harb, J. S. Harris, Jr., and R. N. Zare, *Chem. Phys. Lett.* **290**, 335 (1998).
8. R. W. P. Drever, J. L. Hall, F. V. Kowalski, J. Hough, G. M. Ford, A. J. Munley, and H. Ward, *Appl. Phys. B* **31**, 97 (1983).